Received: 12 September 2018 | Revised: 26 October 2018 | Accepted: 27 October 2018

DOI: 10.1111/jace.16196

Journal of the American Ceramic Society

ORIGINAL ARTICLE

Fractal characterization of ceramic crack patterns after thermal shocks

Fei Qi[1] | **Songhe Meng**[2] | **Fan Song**[3] | **Hao Guo**[4] | **Xianghong Xu**[3] | **Yingfeng Shao**[3] | **Yao Chen**[1]

[1]School of Mechanical and Electric Engineering & Collaborative Innovation Center of Suzhou Nano Science and Technology, Soochow University, Suzhou, China

[2]Science and Technology on Advanced Composites in Special Environment Laboratory, Harbin Institute of Technology, Harbin, China

[3]State Key Laboratory of Nonlinear Mechanics, Institute of Mechanics, Chinese Academy of Sciences, Beijing, China

[4]Jiangsu Provincial Key Laboratory of Advanced Robotics & Robotics and Microsystems Center, Soochow University, Suzhou, China

Correspondence
Hao Guo, Jiangsu Provincial Key Laboratory of Advanced Robotics & Robotics and Microsystems Center, Soochow University, Suzhou, China.
Email: hguo@suda.edu.cn

Funding information
National Natural Science Foundation of China, Grant/Award Number: 11402156, 61503269, 51275326; National Basic Research Program of China, Grant/Award Number: 2015CB655200; Natural Science Foundation of Jiangsu Province, Grant/Award Number: BK20140301; Natural Science Foundation of the Higher Education Institutions of Jiangsu Province, Grant/Award Number: 14KJB130004; Postdoctoral Research Funding of Soochow University, Grant/Award Number: 32317453

Abstract

This work utilized a combination of experimental evidence and fractal geometric method to assess the effect of crack extension concerning the thermal shock on residual strength of ceramics. Sintered alumina (Al_2O_3) ceramic slabs were bundled and quenched in water under different thermal shock temperatures. The fractal dimension of thermal shock crack patterns on the interior surface and the cooled surface was calculated by the Box-counting method. Fracture energy of a fractal pattern of microcracks in quasi-brittle solids was employed to explain the relationship between crack length and fractal dimensions. The results show that if the crack propagation has the same crack length but a larger fractal dimension, it will absorb more fracture energy. The thermal shock crack patterns of Al_2O_3 ceramics with different grain sizes were analyzed, and the smaller grain size ceramic had a higher fractal dimension of crack patterns than the larger one.

KEYWORDS

brittle materials, crack growth, fractal geometry, thermal shock resistance

1 | INTRODUCTION

Structural ceramic materials, including carbides (SiC, ZrC), nitrides (AlN, BN), borides (ZrB_2, HfB_2), oxides (Al_2O_3, ZrO_2) and composites based on these structural ceramics, have high strength, modulus and thermal conductivity, good corrosion resistance, oxidation resistance, and chemical stability.[1] The excellent high-temperature mechanical

performance makes ceramic materials be widely used in the frontier fields, such as thermal insulation structures, hypersonic aerospace vehicles, propulsion systems, thermocouple sheaths, and refractory crucibles. However, the inherent brittleness of ceramic materials makes them particularly susceptible to thermal shock failure, even catastrophic fracture.[2]

More than half a century ago, researchers such as Kingery[3] and Hasselman,[4–6] focused on the critical thermal shock temperature difference, as well as thermal shock fracture and damage resistance parameters. Subsequently, Gupta[7] suggested that the strength degradation and crack propagation depended on the initial strength and grain size of ceramic materials, which supported the view of Hasselman. The relationship between crack extension and thermal shock resistance is always the hot issues. Evans and Charles[8] explored the theory of structural stability of ceramics in severe thermal environments, which gave the criterion for the prevention of crack propagation. In 1967, Davidge[9] used the cutting specimens method to observe interior cracks, in order to investigate the damage mechanism of ceramics in thermal shocks. Bahr[10] modified the experimental procedure of Davidge,[9] and put emphasis on the time-dependent stress intensities due to quenching. He quenched sintered slabs into the water and generated crack patterns at different temperature differences. As researchers intend to discuss cracking as a two-dimensional phenomenon observable on the side faces of samples of small thickness, so at beginning they will not worry about what is going on in the third dimension.[10] The bundled specimens used in the thermal shock experiments will minimize the effect of the third dimensions, which will simplify the problem and be very helpful to investigate the damage mechanism of ceramics in thermal shocks. These crack patterns serve as evidence for a scheme set up with the aim of explaining the variety of ways in which materials respond to thermal load and on the concept of an energy release rate.[11]

Inspired by Bahr's research works, in the last decade, many researchers studied crack patterns after thermal shocks, in order to reveal mechanisms between residual strength and crack characteristics.[12–19] For thin ceramic specimens, Shao[12] conducted thermal shock testing in the temperature range higher than the critical thermal shock temperature difference (ΔT_c) and showed that the depth of long crack was gradually increased in regime III, which supported the standpoint of Davidge[9] and Bahr,[10] although Hasselman had opposite results. Shao[12] considered the influence of long crack depth and density on residual strength offset each other to some extent, which was also revealed from the results of the finite element method. From the experimental aspect, Xu[19] suggested that at the critical point of quench temperature, the crack density and the depth of ceramic bars reached the minimum and the maximum limits, respectively, which provided a quantified relationship between crack density and depth.

The numerical simulation is also introduced to predict crack propagations subjected to thermal shock loading. Jiang[15] utilized a combination of experimental evidence and finite element method, based on the minimum potential energy principle, to assess the mechanism of formation of thermal shock crack patterns in ceramics. By using the similar method, Wu[18] devoted to the size effect and Liu[20] employed thin circular ceramic specimens in thermal shock experiments. In the research of Jiang,[15] Wu[18] and Liu,[20] they do not only reproduce the evolution of crack patterns with regular periodic and hierarchical characteristics during the thermal shock process but also expect to reveal the mechanism forming this kind of patterns. Contemporaneity, Li[16,17] presented a numerical simulation method on the cracking process of ceramic materials, based on a non-local approach to fracture modeling and its finite element implementation. All the simulations mentioned above consider the two-dimensional (2D) structures and plane stress. It is necessary to consider the temperature-dependency of the thermal parameters, dynamics effect, and three-dimensional (3D) structures extension etc., which could be important issues in the future.[17]

For most researches above, even assisted by some software, the crack depth and density obtained from experiments are counted by naked eyes. They are discussed separately from statistical analysis. In addition, some fine cracks cannot be quantified since their complex patterns. Like the cooled surface which contact the quenching water directly and form some net-like patterns. Therefore, the fractal method is employed in this paper in order to provide a method to describe the cracks patterns based on experimental results directly, which is convenient and can obtain the geometrical characteristics of the crack holistically.

Generally, generalized method of cells (GMC), Voronoi diagram finite element model, multi-scale modeling, probabilistic method, and fractal method are applied to characterize material microstructures. Among these methods, the fractal method is adequate for describing irregular, non-uniform and self-similarity characters, like crack propagation, fracture surfaces generation, porous structure and so on. From the pioneering work of Mandelbrot,[21] the fractal nature of real solid fracture surfaces has been confirmed by numerous experimental studies, such as rock, ceramic, concrete, and metal crack surfaces with fractal features. Microcracks and crack distributions have self-similarity at a certain scale,[22] and the critical stress of fractal cracking for brittle and quasi-brittle materials were also discussed sufficiently.[23,24]

This paper is composed according to the following scheme. First, we obtain thermal shock patterns by quenching ceramic slabs. Second, we try to characterize the patterns from the fractal geometry aspect, taking into account

the effect of fractal results on the residual strength of ceramic after thermal shocks. Absorbed energy for microcracks is employed to explain the crack propagation, and the effect of ceramic grain size is also discussed simultaneously.

2 | EXPERIMENT

2.1 | Materials processing

The Al_2O_3 ceramic reported here was processed by Henan Jiyuan Brother Material, Jiyuan, China, with the median particle size 1 μm and the purity >99%, uniaxially pressed at 20 MPa into pellets and subsequently sintered without pressure. The dimension of ceramic bulks was 50 mm in length, 50 mm in width, and 5 mm in thickness. The density of the ceramic was larger than 95% by calculation from measured dimension and weight. Two kinds of alumina were sintered, with the median grain size 10 and 3 μm respectively. The microstructure of Al_2O_3 ceramic was observed using an electron microscope (S-570; Hitachi, Tokyo, Japan).

2.2 | Thermal shock test

Ceramic bulks were cut into slabs of size 5 mm × 10 mm × 50 mm, grounded to obtain smooth parallel faces and chamfered to minimize the effect of stress concentration due to machining flaws (Figure 1A). To prevent access of the coolant to the side faces, the specimen was stacked with another four ceramic slabs, and bound up with Inconel wires (0.4 mm in diameter; Shanghai New Soviet China Special Alloy Material, Shanghai, China), as shown in Figure 1B. The stack was heated in a muffle furnace, with the heating rate of 15°C/min and the holding time of 20 minutes under a preset temperature. Subsequently, the stack was taken out from the muffle furnace and dropped into water (~17°C) immediately. After cooling 10 minutes, the specimen was dried at 80°C for 2 hours, and impregnated

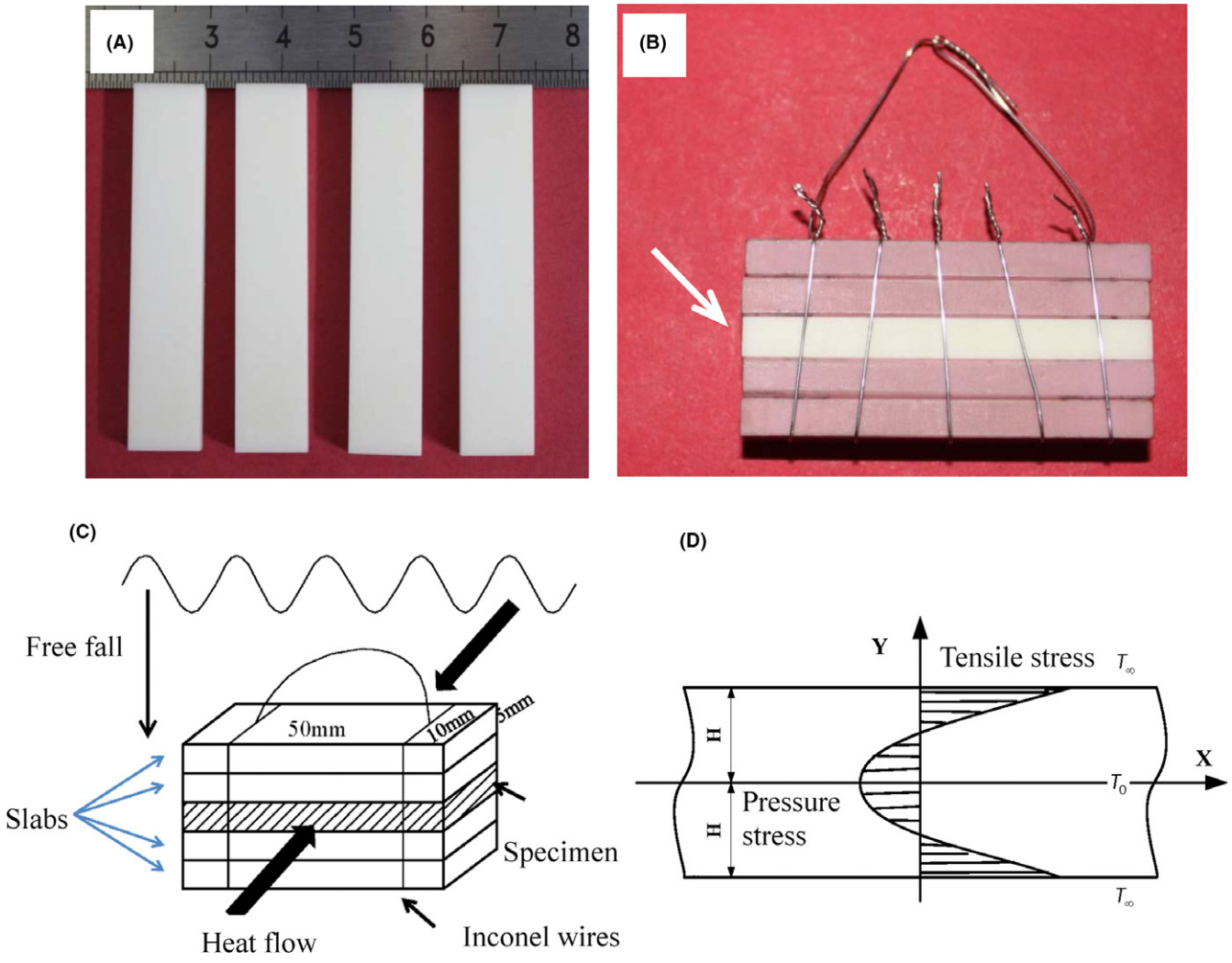

FIGURE 1 A, The Al_2O_3 specimens. B, The specimen covered by ceramic slabs and tightened by Inconel wires. C, The water-quenching experiment schematic diagram. D, Stress distribution of specimen under quenching

with a blue dye. After drying, we obtained the crack patterns. For conciseness, we refer to publication[10,12] where some auxiliary ideas and experimental procedure have been outlined in more detail.

The thermal shock schematic diagram was shown in Figure 1C. Since the stack temperature is much higher than the water before quenching, when it contacts the water, temperature differences will exist between the surface and the interior surface of the specimen, resulting in thermal stress. The stress distribution of the specimen under quenching was shown in Figure 1D. It can be seen that the surface of the specimen is subjected to tensile stress due to cooling shrinkage, but the region nearby the mid-plane of ceramic labs is compressive stress. The surface of the specimen has the maximum tensile stress, so the crack first nucleates on the surface and extends from the surface toward the center of the specimen along the temperature gradient. The stress is largest at the surface and decays with depth.

The flexural strength of the specimens before and after thermal shocks was measured in three-point bending on 5 mm by 10 mm by 50 mm bars, using a 40 mm span and a crosshead speed of 0.5 mm/min. A minimum number of five specimens were measured for per experimental condition.

2.3 | Fractal calculation

There are many mathematical definitions of fractal dimensions, such as the Hausdorff dimension, Box-counting dimension, Self-similarity dimension, and so on. For some classic fractal geometry, like Koch snowflake, these dimensions coincide; however, in general, they are not equivalent.

For the crack patterns, the Box-counting dimension is calculated by the following method. For an object on the plane $\mathbb{R}^2$, the area is discretized by squares with a length of δ, namely box size. Then, count the number of squares ($N(\delta)$) that cover the cracks. Repeat the above processing when δ takes different values from larger to smaller; we can get the following relation:

$$N(\delta) \propto \delta^{-D}. \quad (1)$$

The fractal dimension D is calculated by the linear fit of $\mathrm{In}(N(\delta))$ vs $\mathrm{In}(\delta)$.[23,25]

3 | RESULTS AND DISCUSSIONS

3.1 | Thermal-shock crack patterns

The crack morphology of samples at quenching temperatures of 215, 300, 400, 500, and 600°C was shown in Figure 2. The water bath temperature is 17°C. We scanned morphology of four adjacent faces of a specimen after thermal shocks. The two wider surfaces are named as "interior surfaces" of the specimen (No. 1 and No. 2). The two narrower ones (No. 3 and No. 4) are defined as "surface", which contact with the cool water directly during quenching.

It can be seen from Figure 2B, when T is 215°C, a significant macroscopic crack appears in the specimen. From observation of the length and morphology of the crack

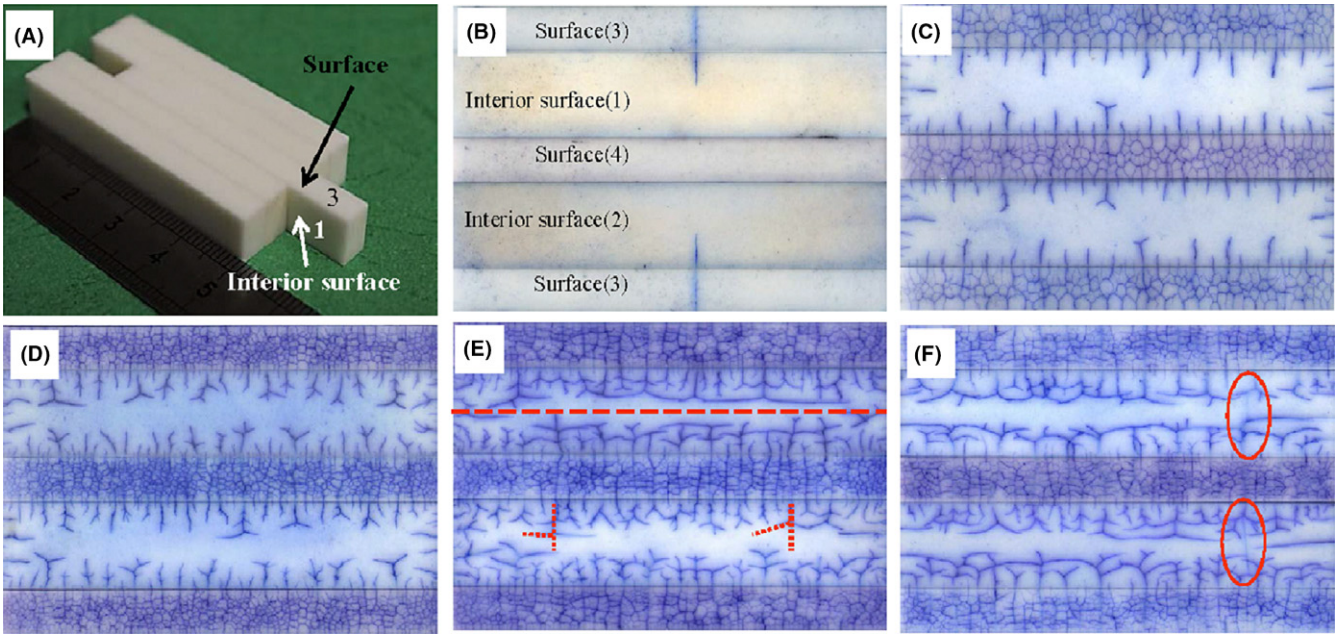

FIGURE 2 A, Indicate the surface and the interior surface of the specimen. Crack patterns in Al_2O_3 specimens with a grain size of 10 μm at quenching temperatures of (B) 215°C, (C) 300°C, (D) 400°C, (E) 500°C, and (F) 600°C, respectively. The water bath temperature is 17°C

generated, it penetrates the entire thickness of the specimen. As sparse cracking in observed at $T = 215$°C while at 210°C there is no cracking at all. From the residual strength of ceramics (Table 1), the bending strength of 10-μm Al_2O_3 reduces to 242.40 MPa at $T = 210$°C, but 77.69 ± 15.11 MPa at $T = 215$°C. Compared with 314.44 ± 17.09 MPa, the room temperature strength of initial specimens, ΔT_c must be situated between 193 and 198°C (water bath temperature is 17°C). In our search, we just observe one crack at critical temperature. Cracks on the cooled surface run preferentially straight between edges. Since ceramics are brittle materials, this crack can be speculated as the principal factor that reduces the strength of the ceramic. This phenomenon is the same with the results of Bahr[10] and Xu,[19] they indicated that the cracks on the surface (No. 3 and No. 4) are straight, and parallel to each other under lower quenching temperatures.

With the thermal shock temperature increasing, the stress changes from mainly uniaxial to mainly plane, as seen from the net-like surface crack patterns from Figure 2C-F. When $T = 300$°C, the number of cracks increases significantly compared with $T = 215$°C (Figure 2C). Since the crack surface is in direct contact with the quenching medium, not only long cracks penetrate through the thickness direction, numerous a large number of fine mesh cracks appears. On the interior surface, the crack spreads along the direction of the temperature gradient. Both long cracks and short cracks exist simultaneously, with hierarchical characteristics. A few long cracks appear bifurcation. A comprehensive view of the interior surface of specimens reveals the existence of a characteristic length affecting the crack length opposite to it: a long crack on one side along with a relatively short crack on the other side. In this figure and direction, that is, a long crack upside along with a relatively short crack on the bottom, and the reverse is also true. This phenomenon is very common. It may be contributed to the thermal filed is not rigid symmetrical for the mid-plane when the specimen dropping into the water, which may be derived from the week fluctuation of water. What is more, near the mid-plane of the specimen, a few long cracks tend to turn to spall.

When T increases to 400°C (Figure 2D), the surface crack is finer and denser. The crack density increases a lot by naked eyes. On interior surfaces, bifurcation phenomenon of long crack increases, and many cracks appear multi-stage crack bifurcation.

As T equal to 500°C, as shown in Figure 2E, it is interesting that the surface crack density of the specimen reduces compared with $T = 400$°C. Most of the long cracks in interior surface bifurcate, but without cracks passing through the mid-plane. The crack bifurcation angle is the angle between the temperature gradient direction and the crack direction after quenching (see the red dotted line in Figure 2E). We found the crack bifurcation angle increasing with larger T, and many angles reach 90° when $T = 500$°C. After the bifurcation, the crack length also increased, and many bifurcation cracks connect with their adjacent cracks.

When the water quenching temperature increase to 600°C (Figure 2F), the crack pattern is similar to 500°C. However, one crack extends through the mid-plane of the interior surface (see the red cycle in Figure 2F). Because the pressure stress is maximal near mid-plane, (Figure 1D). The phenomenon that a crack extends through the mid-plane may be attributed to the inertia of crack propagation. Since the thermal shock is very fierce, and crack propagation is a dynamic process. When T increases from 500 to 600°C, the thermal stress increases during the thermal shock process, and the penetrating crack occurs due to the inertia of the crack propagation.

The strength of 10 μm-Al_2O_3 ceramic fluctuating with quenching temperature (T) shows in Figure 3. When T is 210°C, the ceramic strength begins to decay, but it still retains 77.1% of initial strength at room temperature. This may be the reason that we do not see any cracks on the specimen. However, it is very close to 70%, which it usually seems like the breakdown point of brittle materials in fracture mechanics. The quenching temperature 215°C is regarded as the critical temperature, which residual strength drops rapidly and only retains 24.7% of the initial strength of the bulk ceramic. When we improve quenching temperature to 300, 400, and 500°C, the residual strengths is around 76 MPa without marked variation. Until T increases to 600°C, the strength decreased to 15.23 ± 9.44 MPa, which may be attributed to the generation of a penetrating crack across the mid-plane of the specimen. The strength degradation curve is same with the four stages in thermal shock testing of dense ceramics.[5]

3.2 | Fractal characterization of cracks

From the observation of geometrical morphology and previous studies,[22] we assume the net-like crack patterns on the surface and branch-like crack patterns on the interior

TABLE 1 Room temperature strength of thermally shocked alumina as functions of quenching

Quenching temp. T(°C)	17	200	210	215	220	300	400	500	600
10-μm Al_2O_3 (MPa)	314.44	—	242.40	77.69	85.82	76.06	66.52	75.02	15.23
3-μm Al_2O_3 (MPa)	342.43	343.63	—	—	199.30	69.35	75.10	77.64	75.65

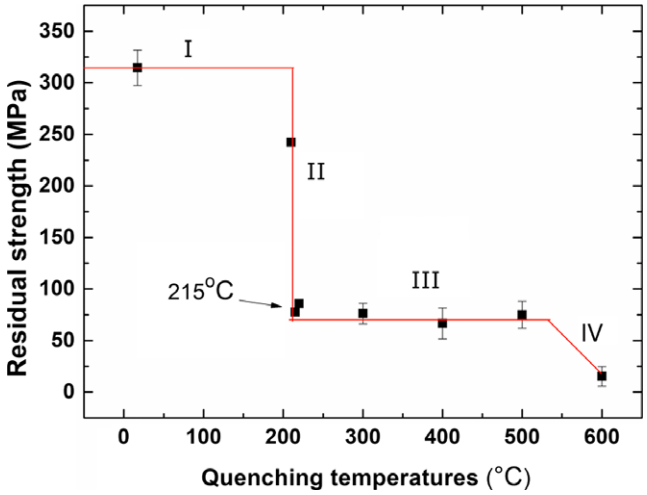

FIGURE 3 Residual strength of 10 μm-Al_2O_3 after quenching. The water bath temperature is 17°C

surface have self-similarity within a certain scale. The box-counting method is employed to calculate the fractal dimension of crack patterns. Before calculation, it is preferable to preprocess the original images: to transform the color image into black and white, means binary image, as shown in Figure 4.

Firstly, the original image is filtered by Gaussian Filter in MATLAB, which removes the interference caused by uneven dyeing or impurities on the surface as much as possible. Then, the image is converted to a grayscale image with a color range of [0, 255], and etched the cracks numerically to make its profile clearly. Finally, according to the histogram of the grayscale, binarize the image, and then transform the grayscale image into black and white. The value of black is zero, which means cracks. In Figure 5, we draw up the preprocessing image of crack patterns after quenching at temperature T of 215, 300, 400, 500, and 600°C, respectively. The preprocessing image ensures a good accuracy in crack patterns, what is more, many fine cracks display faithfully.

Let $\delta = 2^{k-1}$, k = 1,2,3,4, where δ is the length of the "box", which means how many pixels are used to cover a point. Divide the image length by δ to get the relative length (M), and divide the image width by δ to get the relative width (N). Then M multiply N is the box numbers including the whole image. Since the value of cracks is zero (black), count the number of boxes containing zero, then the crack fractal dimension can be calculated by Equation 1.

A remarkable advantage of the fractal method is that the pattern morphology can be described by only one parameter: the fractal dimension, no matter what the complexity of the pattern. Therefore, from the fractal dimension, we can extract the geometry information of cracks easily, and compare them conveniently.

For 10 μm-Al_2O_3, the crack pattern dimensions of the interior surface D_I (No. 1 and No. 2) and the surface D_S (No. 3 and No. 4) after quenching are shown in Table 2. At the critical temperature of 215°C, the fractal dimension of the crack is relatively low, $D_I = 1.0517$ and $D_S = 1.0308$. Since the dimension of a straight line equal to 1.0, and the dimension closed to 1.0 means that the crack spreads almost in a straight line. This is coincident with the experimental results in Figure 2B.

When T increases from 215 to 300°C, both D_I and D_S improved significantly, the growth rate is 28.7% and 42.2% respectively. A large increase in dimension suggests that the cracks increase a lot, as seen in Figure 6. When T = 300°C, a large number of cracks begin to appear (Figure 2C). Compared with D_I, D_S improves much more obviously, attributed to a mass of net-like cracks generate on the surface. The stress is largest on the surface and decays with depth, while the fractal dimension is sensitive to this fine distinction. Previous research has found that, when quenching temperature

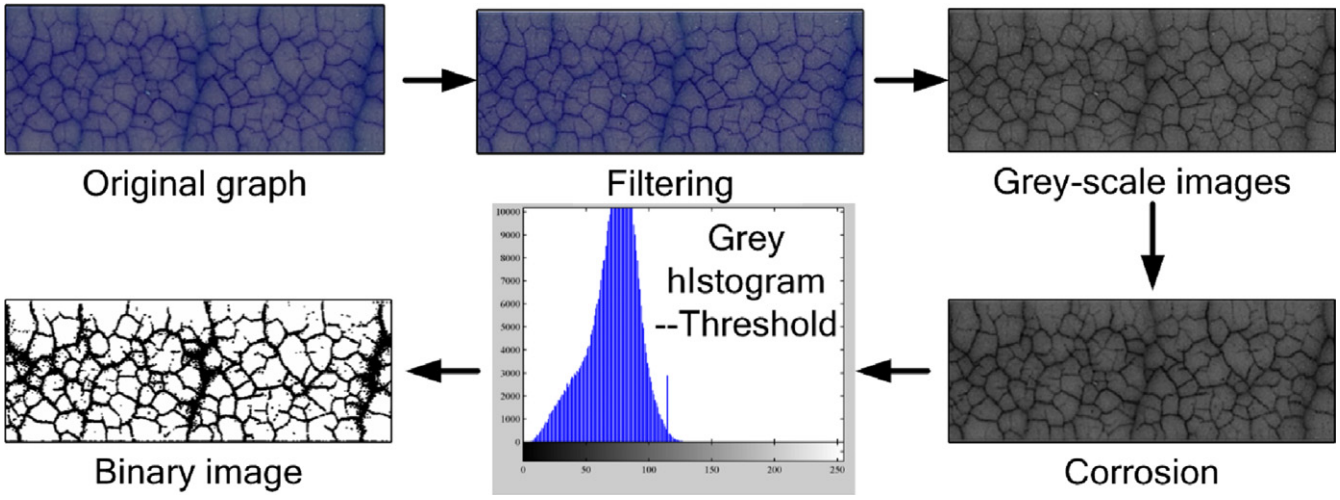

FIGURE 4 Image preprocessing method based on the original crack patterns

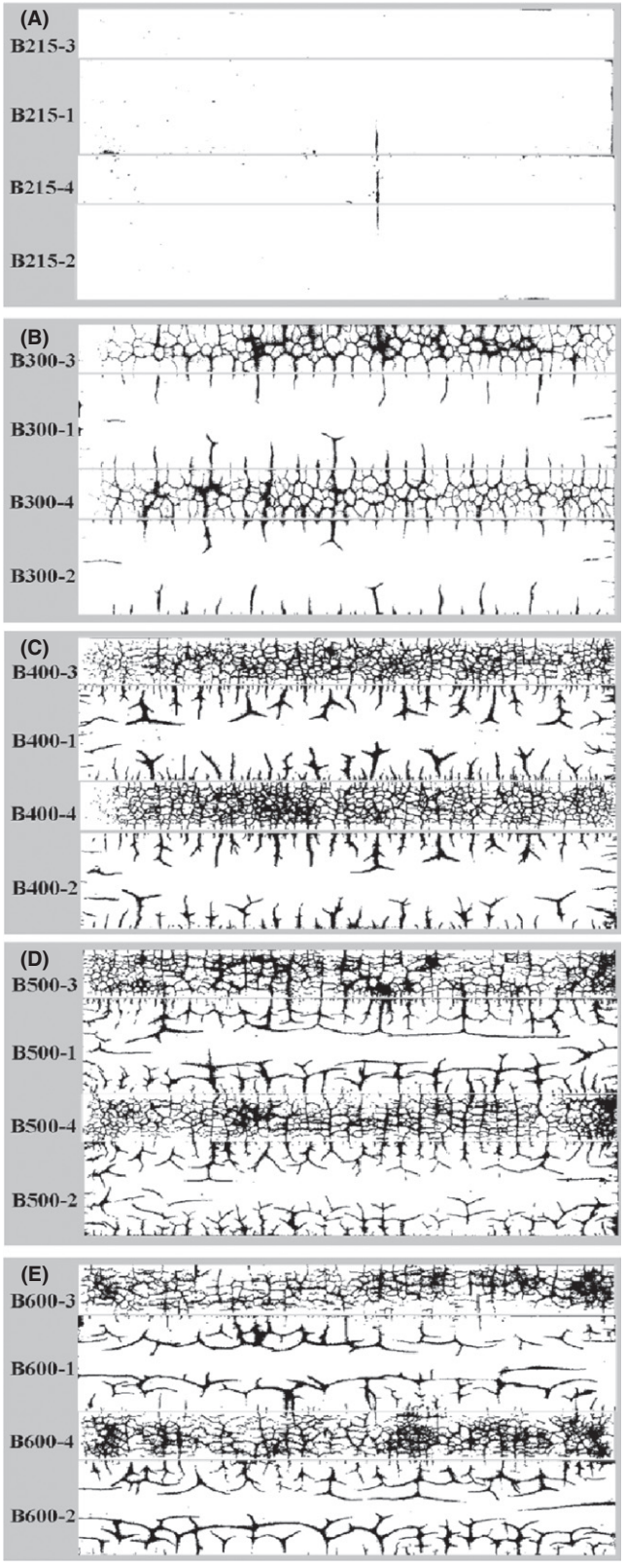

FIGURE 5 Preprocessing images of crack patterns after quenching at the temperature of (A) 215°C, (B) 300°C, (C) 400°C, (D) 500°C, and (E) 600°C, with the water bath temperature 17°C

T just passed critical temperature T_c, the crack depth and the crack density have an opposite tendency.[12,19] That means, although the density of cracks increases at 300°C, the crack depth decreases to a certain extent. That is the reason why the fractal dimension increases a lot, but the residual strength does not change too much from 215 to 300°C.

The crack fractal dimension does not change too much when T increasing from 300 to 400°C, and 400 to 500°C, with the growth rate of D_I 8.98% and −3.02%, as well as, the growth rate of D_S 6.17% and −0.15% (Table 2). It indicates that the proportion of cracks in the ceramics stabilizes at a certain level. Corresponds to the residual strength of the material, the residual strength does not change too much, in addition, it has an opposite trend with fractal dimension growth rate. For 10 μm-Al_2O_3, this trend is identical for all quenching temperatures (Figure 6). The fractal dimension can extract the crack length and density information concurrently. The crack patterns for 300, 400, and 500°C are different, like crack length, density, and bifurcation. But they have similar fractal dimensions and residual strength.

The fractal dimension does not change too much from 500 to 600°C. $D_I = 1.65\%$ and $D_S = 0.46\%$, and the crack pattern is also similar to each other. But the residual strength degrades a lot, which is probably attributed to the penetrating crack. The fracture mechanism may change from 500 to 600°C, and the dimension of surface and interior cracks does not become sensitive to the residual strength in Regime IV. A penetrating crack means the existing of a fracture surface. Therefore, we infer, it may need to develop the fractal dimension method in three-dimensional space in Regime IV in future.

The fractal dimension of the surface is more sensitive than the interior surface when T increases from 215 to 300°C, and its value higher than the interior surface fractal dimension from 300 to 600°C. This may be attributed to the larger thermal stress on the surface (No. 3 and No. 4), which in direct contact with the quenching medium, resulting in the higher crack density than the interior surface (No. 1 and No. 2).

A projection length of the extended fractal curve onto the x-axis (L_0) can be understood by Figure 7, as well as the following equation:

$$L_0 = l_0^D \delta_*^{1-D}, \tag{2}$$

where L_0 is the projection length of the fractal crack, l_0 is the straight crack length, D is the fractal dimension, and δ_* is an elementary piece of fractal crack. In the case of quasi-brittle fracture, the fracture energy, which considers the fractal length (L_0) but not always a straight length (l_0), is more reasonable and closer to real situations.

TABLE 2 Fractal dimensions of crack patterns of Al_2O_3 with grain size 10 μm

Interior surface	D_I	Mean (1,2)	Growth rate (%)	Surface	D_S	Mean (3,4)	Growth rate (%)
B215-1	1.0517	1.0919		B215-3	0.8655	1.0308	
B215-2	1.1320			B215-4	1.1961		
B300-1	1.3481	1.4056	28.73	B300-3	1.4914	1.4656	42.18
B300-2	1.4631			B300-4	1.4398		
B400-1	1.5041	1.5318	8.98	B400-3	1.5324	1.5560	6.17
B400-2	1.5111			B400-4	1.5796		
B500-1	1.4703	1.4856	−3.02	B500-3	1.5711	1.5537	−0.15
B500-2	1.5009			B500-4	1.5363		
B600-1	1.4879	1.5101	1.65	B600-3	1.5418	1.5608	0.46
B600-2	1.5323			B600-4	1.5798		

D_I is the fractal dimension of interior surface (No. 1 and No. 2); D_S is the fractal dimension of surface (No. 3 and No. 4), Figure 2B.

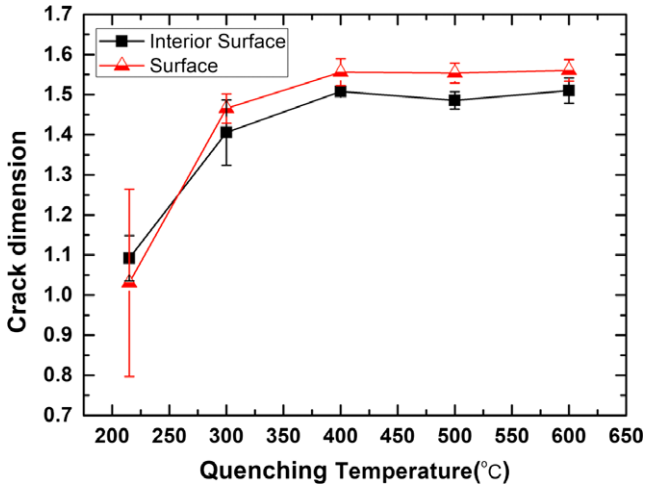

FIGURE 6 For 10 μm-Al_2O_3, the fractal dimensions of interior surface cracks and surface cracks, at quenching temperature of 215, 300, 400, 500, and 600°C respectively. The water bath temperature is 17°C

Borodich[23] studied fracture energy of a fractal pattern of microcracks in quasi-brittle solids. In his research, the effective energy absorbing capacity G_f of an elementary piece δ_* of fractal cracks was introduced. The cracks were viewed as a cluster of elementary crack particles of length δ_*. Therefore, the average of the total amount of $\langle W\rangle$ of absorbed energy for the microcracks pattern is the following formula:

$$\langle W\rangle \sim \begin{cases} G_f\delta_*(x/\delta_*)^D, & \delta_*<x<\Delta \\ G_f\delta_*(\Delta/\delta_*)^D(x/\Delta), & \Delta<x \end{cases} \quad (3)$$

where Δ is some length that fractal features of the crack are displayed for $\delta_* \le \Delta$. For $x > \Delta$, each piece of the crack of length Δ absorbs the same value of energy. In this formula, we know $(x/\delta_*) > 1$, $(\Delta/\delta_*) > 1$, and $1 < D < 2$. While the crack grows, the energy absorbed by elastic deformation is far less than its plastic deformation. G_f is approximately equal to the energy absorbed by plastic deformation. That is to say, if G_f is same in a quasi-brittle fracture, the absorbed energy $\langle W\rangle$ will increase along with the increase in crack length x and dimension D.

In our experiment, if the crack propagation has the same crack length but a larger fractal dimension, it will absorb more energy. In other words, for a given absorbed energy, a larger fractal dimension will be accompanied with a shorter crack length. What is more, from the absorbed energy for the microcracks pattern (in Equation 3), the total amount $\langle W\rangle$ of absorbed energy is an average quantity, therefore, the crack length will include all the cracks in the pattern, but not like the crack length counted in previous studies of Shao[12] and Jiang,[15] considering every crack length independently.

Since the complicated crack patterns, previous studies never considered the surface carks so much (No. 3 and No. 4). We provide a fractal mothed here to characterize their geometrical morphology and hope to analyze the effect of crack extensions from a novel aspect. For examining the effectiveness of this method, we employ another Al_2O_3 ceramics with median grain size 3 μm in following studies.

3.3 | Effect of grain sizes

Gupta[7] found that the strength decay and crack propagation in Al_2O_3 ceramics depend on the initial strength and grain size of the material. In order to study the effect of grain size on the thermal shock resistance, we also considered the Al_2O_3 ceramic with median grain size 3 μm after quenching. The crack pattern of the surface and interior surface of 3 μm-Al_2O_3 is preprocessed. Crack pattern details can be founded in the Appendix 1. The fractal dimensions of 3 μm-Al_2O_3 were calculated and compared with that of 10 μm-Al_2O_3 in Figure 8.

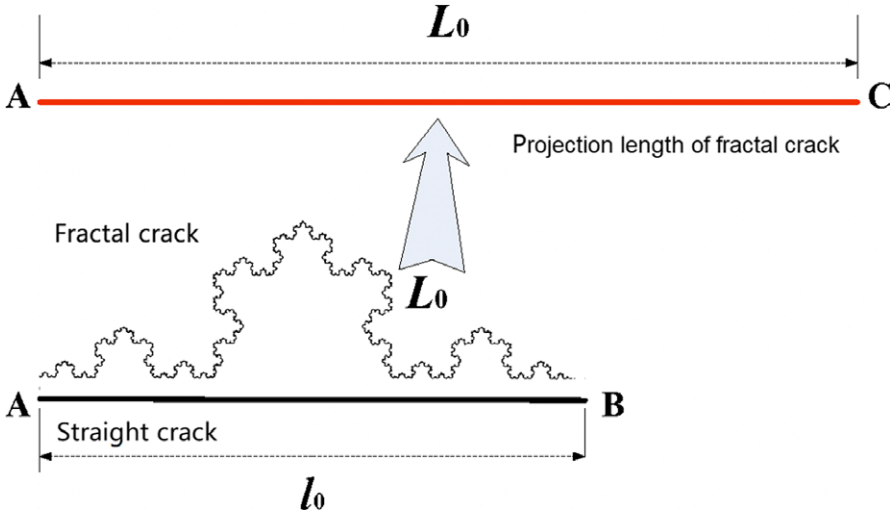

FIGURE 7 Projection length of the fractal crack

From the comparisons of these ceramics, the fractal dimensions of the surface cracks and interior surface cracks of 3 μm-Al_2O_3 ceramics are all larger than that of 10 μm-Al_2O_3. For polycrystalline aluminas with grain sizes of 3 and 10 μm, the smaller the grain size was, the larger the fractal dimension of the crack after thermal shocks.

For 3 μm-Al_2O_3, as can be seen from Table 3, from $T = 220$-300°C, the dimension growth rate of the surface (D_S) is 29.13%, much higher than the others. Therefore, we estimate the critical temperature is more than 220°C but very close to 220°C. The crack pattern and residual strength also confirm this result: it is only two cracks on the surface and the residual strength under $T = 220$°C is 199.30 MPa, which maintains 41.8% of initial strength (Table 1). This phenomenon is because of brittle instinct quality of ceramics. When the thermal shock temperature T is nearby the critical temperature T_c, the crack propagation is unstable, as well as the strength data is also highly dispersible. Many previous studies have the same viewpoint and the details can be found in the research of Bahr.[10]

Some experienced researchers can infer the critical temperature difference of ceramics from the crack morphology after thermal shocks, which inextricably linked to the numerous experimental results between crack patterns and residual strengths. The fractal geometry method is also based on the premise that it is desirable to reveal fracture mechanism from the crack morphology.

When quenching temperature exceeds critical temperature, from 220 to 300°C, the residual strength of 3 μm-Al_2O_3 ceramics decays rapidly, and the cracks increase in quantity, resulting in an increase in crack fractal dimension. This phenomenon is the same as 10 μm-Al_2O_3. When quenching temperature rises from 300 to 600°C, the residual strength does not change significantly, which is consistent with Hasselman's classical thermal shock theory.[26] The

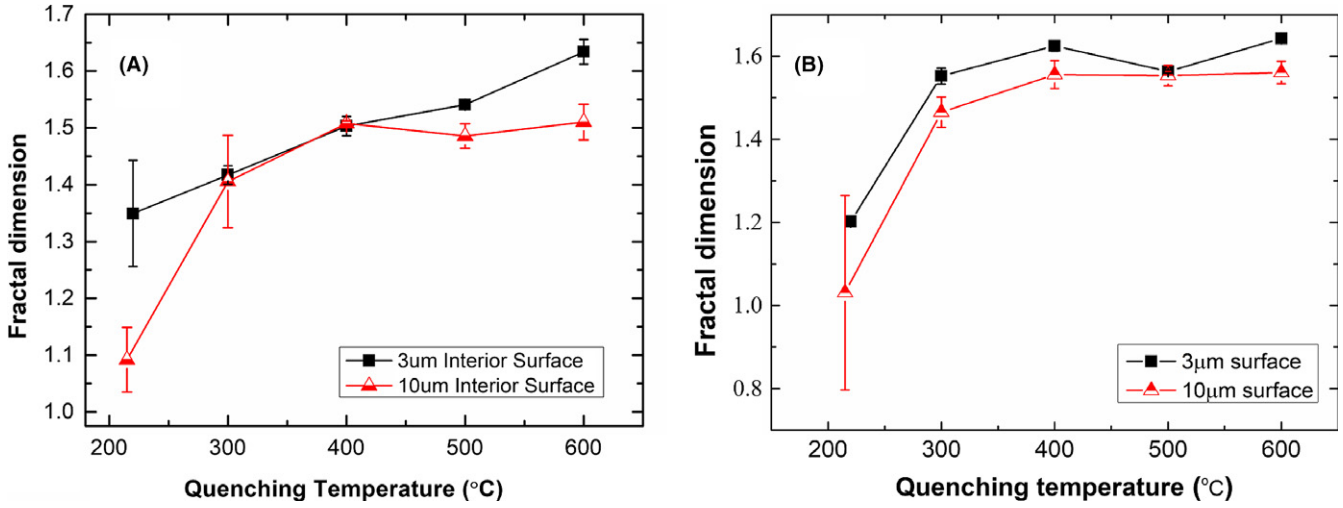

FIGURE 8 Fractal dimensions of (A) interior surface cracks and (B) surface cracks for 3 μm-Al_2O_3 and 10 μm-Al_2O_3

TABLE 3 Fractal dimensions of crack patterns of Al_2O_3 with grain size 3 μm

Interior surface	D_I	Mean (1,2)	Growth rate (%)	Surface	D_S	Mean (3,4)	Growth rate (%)
A220-1	1.2832	1.3493		A220-3	1.2013	1.2024	
A220-2	1.4154			A220-4	1.2034		
A300-1	1.4055	1.4170	5.02	A300-3	1.5392	1.5526	29.13
A300-2	1.4285			A300-4	1.5661		
A400-1	1.5151	1.5031	6.08	A400-3	1.6341	1.6251	4.66
A400-2	1.4910			A400-4	1.6160		
A500-1	1.5447	1.5408	2.51	A500-3	1.5660	1.5635	-3.78
A500-2	1.5368			A500-4	1.5610		
A600-1	1.6493	1.6338	6.04	A600-3	1.6467	1.6431	5.09
A600-2	1.6183			A600-4	1.6395		

D_I is the fractal dimension of interior surface (No. 1 and No. 2); D_S is the fractal dimension of surface (No. 3 and No. 4).

fractal dimensions of surface cracks are 1.5526, 1.6251, 1.5635, and 1.6431, respectively, which change slightly. The dimension of the interior surface increases gradually from 220 to 600°C. When $T = 600$°C, no penetrating cracks in the material is observed, and the residual strength still maintains 75.65 ± 10.77 MPa.

For polycrystalline aluminas with grain sizes of 3 and 10 μm, the strength remains constant up to the critical fracture temperature (Table 1). The initial strength of 3 μm-Al_2O_3 and 10 μm-Al_2O_3 is 342.43 ± 3.15 MPa and 314.44 ± 17.09 MPa, respectively. The initial strength of Al_2O_3 decreases with increasing grain size, which is coincident with Gupta.[7] The critical temperature difference of 3 μm-Al_2O_3 is a little bit higher than that of 10 μm-Al_2O_3. But the grain size difference between these two materials is not so large, which lead to less distinguish of their crack fractal dimensions, critical temperatures, and residual strengths. Therefore, we suspect that reducing or increasing the grain size in the 10 μm range has some effect on the original strength of alumina, but does not make much sense for the improvement of thermal shock performance.

4 | CONCLUSIONS

This work utilized a combination of experimental evidence and fractal geometric method to assess the effect of crack extension concerning the water-quenching on residual strength of brittle materials. The main findings are:

1. The residual strength after thermal shocks is rapidly degraded when a macroscopic crack generated in 10 μm-Al_2O_3 ceramic. As quenching temperature rising from 300 to 600°C, the crack patterns of interior surface demonstrate regular periodic, hierarchical and bifurcate characteristics. The residual strength after critical temperature does not show marked variation until a penetrating crack appears across the mid-plane of the specimen when $T = 600$°C.
2. The fractal dimension of crack patterns after thermal shocks is calculated by the Box-counting method. Even some fine and complex cracks on the surface can be characterized faithfully. The fractal dimension is sensitive to the crack pattern variation under different thermal shock temperatures. Fracture energy of a fractal pattern of microcracks in quasi-brittle solids[23] was employed to explain the relationship between crack length and fractal dimensions. If the crack propagation has the same crack length but a larger fractal dimension, it will absorb more energy.
3. For comparison and verification, the Al_2O_3 ceramics with grain size 3 μm was analyzed by calculating the fractal dimension of crack patterns after quenching. We found the smaller grain size ceramics had a higher fractal dimension of crack patterns than the larger one.
4. The crack bifurcation phenomenon was fierce along with the increasing of thermal shock temperatures. It is interesting that its geometrical morphology is branch-like which has a fractal characteristic. We find the bifurcation angles have some statistical regularity, which is helpful to predict the residual statistical strength after thermal shocks. This is also worth considering in future combined with the thermal stress distribution and energy release rate.

ACKNOWLEDGMENT

The authors acknowledge the financial support from the following research grants: National Natural Science Foundation of China (Grant Nos.11402156, 61503269, 51275326); National Basic Research Program of China (Grant No. 2015CB655200); Natural Science Foundation of Jiangsu Province (Grant No. BK20140301); Natural Science Foundation of the Higher Education Institutions of Jiangsu

Province (Grant No. 14KJB130004); Postdoctoral Research Funding of Soochow University (Grant no. 32317453). Fei Qi is thankful, in particular, for the discussion and the valued suggestion from Professor Shigeo Kotake, in Graduate School of Engineering, Mie University.

ORCID

Fei Qi http://orcid.org/0000-0001-6170-4691

REFERENCES

1. Huang Y, Wang CA. *Multiphase Composite Ceramics with High Performance*. Beijing: Tsinghua University Press; 2008.
2. Wang H, Singh RN. Thermal shock behaviour of ceramics and ceramic composites. Int Mater Rev. 1994;39(6):228–44.
3. Kingery WD. Factors affecting thermal stress resistance. J Am Ceram Soc. 1955;38(1):3–15.
4. Hasselman DPH. Thermal shock by radiation heating. J Am Ceram Soc. 1963;46(5):229–33.
5. Hasselman DPH. Strength behavior of polycrystalline alumina subjected to thermal shock. J Am Ceram Soc. 1970;53(9):490–5.
6. Hasselman DPH. Elastic energy at fracture and surface energy as design criteria for thermal shock. J Am Ceram Soc. 1963;46 (11):535–40.
7. Gupta TK. Strength degradation and crack propagation in thermally shocked Al_2O_3. J Am Ceram Soc. 1972;55(5):249–53.
8. Evans AG, Charles EA. Structural integrity in severe thermal environments. J Am Ceram Soc. 1977;60(1–2):22–8.
9. Davidge RW, Tappin G. Thermal shock and fracture in ceramics. Trans Br Ceram Soc. 1976;66(8):405–22.
10. Bahr HA, Fischer G, Weiss HJ. Thermal-shock crack patterns explained by single and multiple crack propagation. J Mater Sci. 1986;21(8):2716–20.
11. Bahr HA, Weiss HJ, Maschke HG, Meissner F. Multiple crack propagation in a strip caused by thermal shock. Theor Appl Fract Mec. 1988;10(3):219–26.
12. Shao Y, Zhang Y, Xu X, Zhou Z, Li W, Liu B. Effect of crack pattern on the residual strength of ceramics after quenching. J Am Ceram Soc. 2011;94(9):2804–7.
13. Shao Y, Du R, Wu X, Song F, Xu X, Jiang C. Effect of porosity on the crack pattern and residual strength of ceramics after quenching. J Mater Sci. 2013;48(18):6431–6.
14. Shao Y, Liu B, Wang X, Li L, Wei J, Song F. Crack propagation speed in ceramic during quenching. J Eur Ceram Soc. 2018;38 (7):2879–85.
15. Jiang CP, Wu XF, Li J, Song F, Shao YF, Xu XH, et al. A study of the mechanism of formation and numerical simulations of crack patterns in ceramics subjected to thermal shock. Acta Mater. 2012;60(11):4540–50.
16. Li J, Song F, Jiang C. A non-local approach to crack process modeling in ceramic materials subjected to thermal shock. Eng Fract Mech. 2015;133:85–98.
17. Li J, Song F, Jiang C. Direct numerical simulations on crack formation in ceramic materials under thermal shock by using a non-local fracture model. J Eur Ceram Soc. 2013;33(13–14):2677–87.
18. Wu X, Jiang C, Song F, Li J, Shao Y, Xu X, et al. Size effect of thermal shock crack patterns in ceramics and numerical predictions. J Eur Ceram Soc. 2015;35(4):1263–71.
19. Xu XH, Tian C, Sheng SL, Lin ZK, Song F. Characterization of thermal-shock cracks in ceramic bars. Sci China Phys Mech Astron. 2014;57(12):2205–8.
20. Liu Y, Wu X, Guo Q, Jiang C, Song F, Li J. Experiments and numerical simulations of thermal shock crack patterns in thin circular ceramic specimens. Ceram Int. 2015;41(1):1107–14.
21. Mandelbrot BB, Passoja DE, Paullay AJ. Fractal character of fracture surfaces of metals. Nature. 1984;308(5961):721–2.
22. Barenblatt GI, Botvina LR. Similarity methods in the mechanics and physics of fracture. Sov Mater Sci. 1986;22(1):52–7.
23. Borodich FM. Some fractal models of fracture. J Mech Phys Solids. 1997;45(2):239–59.
24. Borodich FM. Fractals and fractal scaling in fracture mechanics. Int J Fract. 1999;95(1/4):239–59.
25. Amada S, Yamada H. Introduction of fractal dimension to adhesive strength evaluation of plasma-sprayed coatings. Surf Coat Technol. 1996;78(1–3):50–5.
26. Hasselman DPH. Unified theory of thermal shock fracture initiation and crack propagation in brittle ceramics. J Am Ceram Soc. 1969;52(11):600–4.

How to cite this article: Qi F, Meng S, Song F, et al. Fractal characterization of ceramic crack patterns after thermal shocks. *J Am Ceram Soc*. 2018;00:1–12. https://doi.org/10.1111/jace.16196

APPENDIX 1

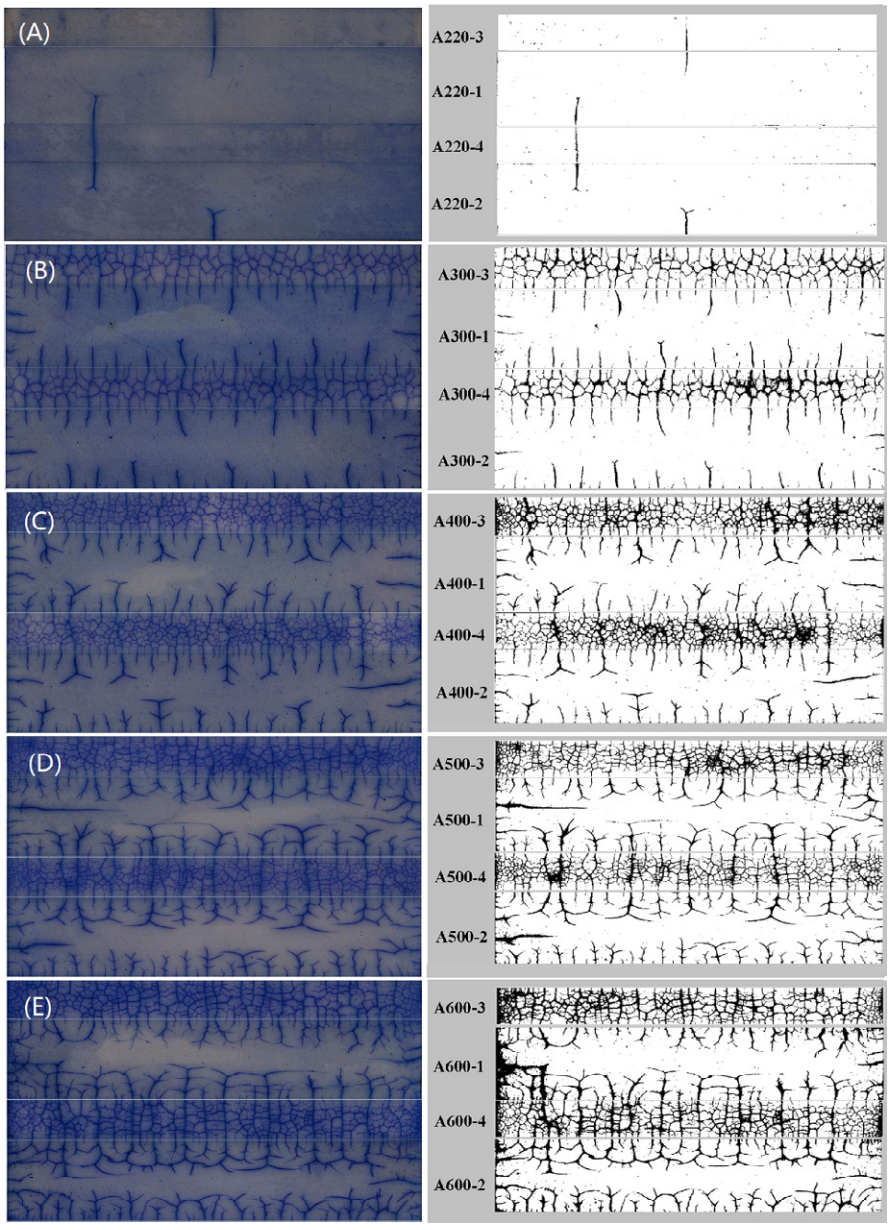

FIG. A1 Crack patterns of 3 μm-Al_2O_3 after thermal shock at the temperature of (A) 220°C, (B) 300°C, (C) 400°C, (D) 500°C, and (E) 600°C, with the water bath temperature 17°C